

## Cross Section Measurements in the $^{54}\text{Cr}(p, \gamma)^{55}\text{Mn}$ Reaction

R. J. Wilkinson,<sup>A</sup> S. R. Kennett,<sup>A</sup> Z. E. Switkowski,<sup>A, B</sup> D. G. Sargood<sup>A</sup>  
and F. M. Mann<sup>C</sup>

<sup>A</sup> School of Physics, University of Melbourne, Parkville, Vic. 3052.

<sup>B</sup> Present address: Kodak Research Laboratories, Kodak (Australasia), Pty Ltd, P.O. Box 90, Coburg, Vic. 3058.

<sup>C</sup> Hanford Engineering and Development Laboratory, Richmond, Washington, U.S.A. 99352.

### Abstract

Cross sections for production of individual  $\gamma$  rays in the  $^{54}\text{Cr}(p, \gamma)^{55}\text{Mn}$  reaction have been measured over the proton energy range 1.0–3.8 MeV. Gamma-ray yields are observed to fall by factors of between 5 and 10 at the crossing of the neutron threshold for a proton bombarding energy of 2.2 MeV. Statistical model calculations with global parameter sets successfully account for the dramatic effect of neutron competition on the  $(p, \gamma)$  cross section, and at the same time correctly predict the  $^{54}\text{Cr}(p, n)^{54}\text{Mn}$  reaction cross section.

### Introduction

As part of a continuing program of  $(p, \gamma)$  cross section measurements for intermediate mass nuclei being carried out by the School of Physics, University of Melbourne (Switkowski *et al.* 1978*a*, 1978*b*; Solomon and Sargood 1978; Kennett *et al.* 1979), we present here studies of the  $^{54}\text{Cr}(p, \gamma)^{55}\text{Mn}$  reaction. The yields of individual  $\gamma$  rays deexciting low-lying bound states of  $^{55}\text{Mn}$  have been measured for proton energies around the  $(p, n)$  threshold. Measurements such as these have provoked considerable interest in recent years, especially in those cases where the opening of a new and strongly competing reaction channel introduces an abrupt change in the energy dependence of already open reaction channels. The original report of a spectacular cusp in the energy dependence of the  $^{64}\text{Ni}(p, \gamma)^{65}\text{Cu}$  reaction (Mann *et al.* 1975) has led to further work at Caltech (Fowler 1976, 1978; Zyskind *et al.* 1977, 1978, 1979) in parallel with the Melbourne program.

The change in reaction cross section, when a competing reaction channel opens, can show up as gross structure in an otherwise smooth yield curve, which may provide a stringent test for Hauser-Feshbach statistical model codes. Switkowski *et al.* (1978*b*; see also references therein) have discussed the importance of such models in current theoretical and technological problems. The most spectacular competition effects occur at the crossing of neutron thresholds for those cases in which the daughter nucleus can be readily produced by s-wave neutrons and the total number of open channels is small. Fig. 1 shows a partial energy level scheme for  $^{54}\text{Cr}+p$  reactions. Although s-wave neutron emission to the two lowest  $^{54}\text{Mn}$  states follows only d-wave proton capture, preliminary calculations by Woosley *et al.* (1975) exhibited a deep cusp in the computed  $(p, \gamma)$  cross section at the opening of the neutron channels. We therefore undertook a study of the  $^{54}\text{Cr}(p, \gamma)^{55}\text{Mn}$  reaction with the aim of comparing the experimental results with the predictions of statistical model calculations,

using global optical-model and level-density parameter sets. As the present investigation was drawing to completion, the results of a similar investigation at Caltech were published by Zyskind *et al.* (1978). The present measurements are compared with these published Caltech data below.

## Experimental Details

### *Targets*

Targets of chromium metal ( $\sim 1 \text{ mg cm}^{-2}$  thick) were prepared, using a technique similar to that of Kuehn *et al.* (1972), by electroplating from a solution containing  $\text{Cr}_2\text{O}_3$  onto clean surgical grade 0.25 mm thick tantalum. The  $\text{Cr}_2\text{O}_3$  was isotopically enriched in  $^{54}\text{Cr}$  to 94.1% (with  $^{50}\text{Cr}$  comprising 0.11%,  $^{52}\text{Cr}$  comprising 4.01% and  $^{53}\text{Cr}$  comprising 1.79%). The target thickness, which was determined by direct weighing of the deposited chromium and was  $\sim 85 \text{ keV}$  at the bombarding energy of the neutron threshold, was chosen to be thick enough to average over hundreds of compound nucleus resonances (Kailas *et al.* 1975) and yet be thin enough to allow observation of the gross structure of the yield curve, namely the cusp.

The target thickness was shown to be macroscopically uniform to 3% from observations of the 1529 keV  $\gamma$ -ray yield from the  $^{54}\text{Cr}(p, \gamma)^{55}\text{Mn}$  reaction during a scan of the target with a 2 MeV proton beam collimated to 2 mm diameter. However, inspection of the target surface with an optical microscope suggested a nonuniform grainy topology of characteristic linear dimension  $\sim 100 \mu\text{m}$ . This microscopic roughness was attributed to the pretreatment of the tantalum substrate by sandblasting, a procedure which had been found essential in order to ensure good adhesion of the electroplated chromium.

As it was considered prudent to perform several independent analyses of target thickness (including use of Rutherford backscattering) an alternative target making scheme, suitable for the fabrication of uniform thin chromium films on flat substrates, was used. To this end, spectroscopic grade elemental chromium of natural isotopic composition (with  $^{54}\text{Cr}$  comprising 2.36%) was evaporated from a tungsten boat onto a cleaned smooth tantalum substrate. The thickness of this target, which was verified to be optically smooth, was determined from the mass difference before and after evaporation to be  $1070 \pm 70 \mu\text{g cm}^{-2}$ . This target was then bombarded by 3 MeV protons, and its thickness was independently inferred from the backscattered ( $\theta = 140^\circ$ ) spectrum by analysing the backscattered proton peak area and also the shift in the tantalum edge when compared with a standard tantalum target. From these analyses, the chromium thickness was found to be  $950 \pm 100 \mu\text{g cm}^{-2}$ , in good agreement with the more precise mass difference value, which was then adopted. It should be noted that investigation of the target composition by backscattering of protons and of 4 MeV  $\alpha$  particles indicated no evidence of oxygen, or other light elements, at levels sufficient to invalidate the analysis procedure. This natural chromium target was used to obtain absolute  $^{54}\text{Cr}(p, \gamma)$  cross sections.

### *Yield Curve Measurement*

The  $^{54}\text{Cr}$ -enriched target and a quartz disc for beam inspection were mounted on a linear motion drive and contained within a stainless steel chamber, which was maintained at a pressure of  $\sim 10^{-6} \text{ Pa}$  by ion pumping. Proton beams were delivered by the University of Melbourne 5U Pelletron accelerator and impinged on the target



was measured over the energy range 1.0–3.8 MeV in 50 keV steps. At each bombarding energy, spectra were recorded for 100  $\mu\text{C}$  of incident charge with a 4096 channel ADC and PDP 11/40 computer, and were stored on magnetic tape for off-line analysis.

In a separate series of runs on the natural chromium target of calibrated thickness,  $\gamma$ -ray spectra were acquired (for the same target-detector configuration as for the enriched  $^{54}\text{Cr}$  target) at proton energies of 1.9, 2.0, 2.1 and 2.2 MeV for an incident charge of 1300  $\mu\text{C}$  per point. Although the  $\gamma$ -ray spectrum was complex owing to reactions with other more abundant chromium isotopes, the 1529 keV photopeak, characteristic of  $^{54}\text{Cr}(p, \gamma)$  reactions, was unambiguously resolved, and its area could be determined to a statistical precision of  $\pm 6\%$ . Following a measurement of Ge(Li) detector efficiency using calibrated sources, the absolute 1529 keV  $\gamma$ -ray production cross section was readily determined, since the target thickness was known. The relative yield measurements with the enriched  $^{54}\text{Cr}$  target were then normalized to the absolute 1529 keV  $\gamma$ -ray production cross section.

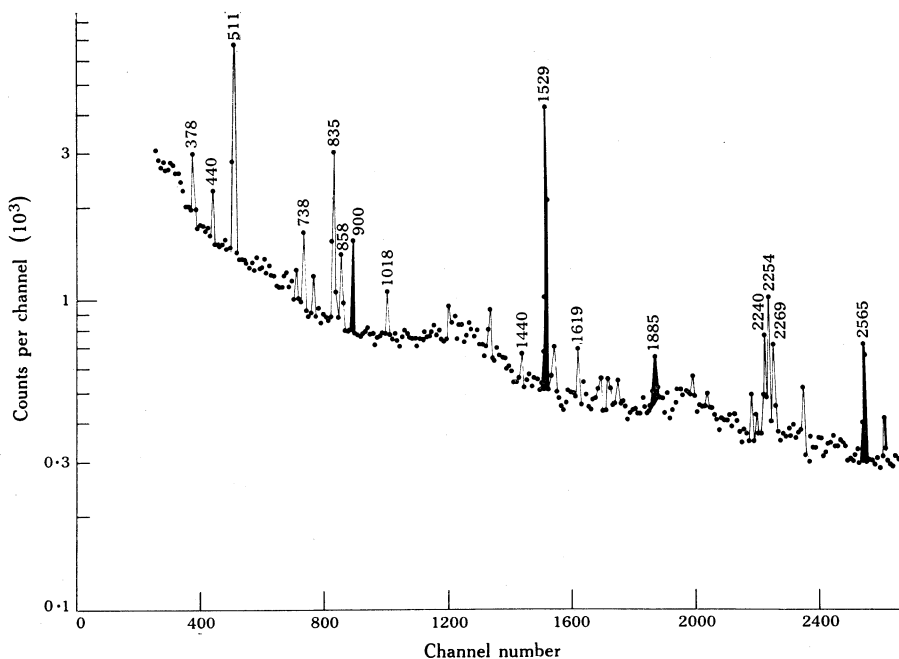


**Fig. 2.** Portion of a  $\gamma$ -ray spectrum for the  $^{54}\text{Cr}(p, \gamma)^{55}\text{Mn}$  reaction taken at  $E_p = 2$  MeV. The spectrum was acquired for an integrated current of 100  $\mu\text{C}$ . Every eighth channel is plotted except near the peaks, where the channel with maximum counts is also shown. Gamma-ray peaks at 378, 835, 1440 and 1619 keV arise from proton-induced reactions on the 4%  $^{52}\text{Cr}$  in the target. The 440 keV line is produced by the contaminant  $^{23}\text{Na}(p, p'\gamma)$  reaction. All other photopeaks labelled by their energies in keV are attributed to the  $^{54}\text{Cr}(p, \gamma)^{55}\text{Mn}$  reaction. Excitation functions for the four shaded peaks are shown in Fig. 3.

## Results and Discussion

A  $\gamma$ -ray spectrum typical for bombarding energies below the (p, n) threshold for  $^{54}\text{Cr}$  is shown in Fig. 2. The spectrum is characterized by a multiplicity of photopeaks, most of which may be positively identified with  $^{54}\text{Cr}(p, \gamma)^{55}\text{Mn}$  reactions. Strong lines are also evident for proton-induced reactions on the 4%  $^{52}\text{Cr}$  and the ubiquitous

$^{23}\text{Na}(p, p'\gamma)^{23}\text{Na}$  reaction arising from sodium contamination in the electrodeposited target. The experimental cross section (points) as a function of the proton energy is plotted in Fig. 3 for four of the stronger  $^{54}\text{Cr}(p, \gamma)^{55}\text{Mn}$  reaction  $\gamma$  rays. These  $\gamma$  rays correspond to transitions between low-lying bound states of  $^{55}\text{Mn}$  (see Fig. 1). The 1529, 1885 and 2565 keV  $\gamma$  rays are the final stages of cascades from  $^{55}\text{Mn}$  resonances populated by proton capture, while the 900 keV  $\gamma$  ray is the transition between the 2429 and 1529 keV states. It is anticipated that these  $\gamma$  rays will have highly damped angular distributions arising from the summation over many resonances, each of different  $J^\pi$  and cascade structure, and that these angular distributions will be further attenuated by the large solid angle subtended by the Ge(Li) detector. The uncertainty in the present data is estimated to be  $\pm 15\%$ .

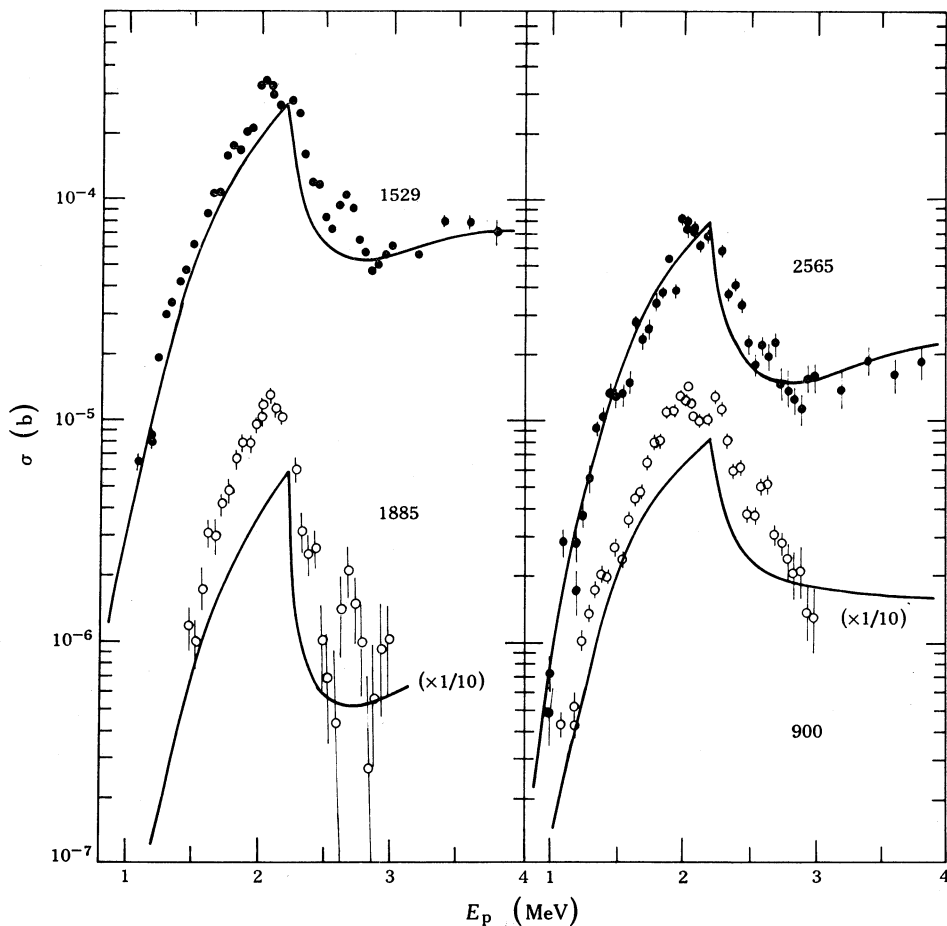


**Fig. 3.** Comparison between experimental data (points) and statistical model calculations (curves) for the proton energy  $E_p$  dependence of the cross section  $\sigma$  for (left) the 1529 and 1885 keV  $\gamma$  rays and (right) the 2565 and 900 keV  $\gamma$  rays from the  $^{54}\text{Cr}(p, \gamma)^{55}\text{Mn}$  reaction. Where shown, experimental error bars reflect statistical uncertainties. The first (p, n) threshold occurs at  $E_p = 2.20$  MeV.

The excitation functions for the individual  $\gamma$  rays exhibit similar features. As the proton energy is increased up the Coulomb barrier, the cross sections increase rapidly until the first (p, n) threshold is reached near  $E_p = 2.2$  MeV. Thereafter the

cross sections plummet, falling by factors of up to 10 for an increase of proton energy of only several hundred keV. Such dramatic threshold phenomena have been seen in some other  $(p, \gamma)$  reactions, particularly  ${}^{64}\text{Ni}(p, \gamma){}^{65}\text{Cu}$  (Mann *et al.* 1975), and they have been somewhat inaccurately labelled 'Wigner cusps' as a result of Wigner's (1948) pioneering calculations which, however, addressed phenomena involving only isolated resonances (W. A. Fowler, personal communication).

An interesting feature of the experimental data is the structure in the form of three peaks near  $E_p = 2.0, 2.3$  and  $2.6$  MeV. The experimental widths of these peaks appear to reflect only the energy thickness of the target. These peaks are attributed to the influence of the lowest  $T = 7/2$  states in  ${}^{55}\text{Mn}$  which carry the isobaric analogue strength of the ground, first-excited and third-excited states of  ${}^{55}\text{Cr}$ , with  $J^\pi$  values of  $3/2^-$ ,  $1/2^-$  and  $3/2^-$  respectively. The  $T = 7/2$  states in  ${}^{55}\text{Mn}$  would be expected to have much larger proton widths to the ground state of  ${}^{54}\text{Cr}$  than would the  $T = 5/2$  states in which they are embedded. Consequently these isobaric analogue resonances (IAR), previously identified by Moses *et al.* (1971), should be conspicuously superimposed upon a smoothly varying  $(p, \gamma)$  compound statistical yield. The analogue of the second-excited state of  ${}^{55}\text{Cr}$  would also be expected to have a large proton reduced width but, since it has  $J^\pi = 5/2^-$  or  $7/2^-$  (Bock *et al.* 1965), f-wave proton capture would be needed to populate it, whereas the other three states are populated by p-wave proton capture. Accordingly, no structure is seen that corresponds to this state. The decays of the two IARs at energies above the neutron threshold differ from the decay of the subthreshold resonance because, in the absence of isospin mixing, neutron emission from the  $T = 7/2$  states to the ground and low-lying states of  ${}^{54}\text{Mn}$ , which have  $T = 2$ , is isospin forbidden. The  $\gamma$ -ray yield from the  $T = 5/2$  states is therefore depleted much more by the opening of the neutron channels than is that from the  $T = 7/2$  states. Hence a  $T = 7/2$  state may provide a larger fraction of the total  $\gamma$ -ray yield just above the neutron threshold than does one just below. In the statistical model calculations (such as are described in the following section), it is customary to assume complete isospin mixing, thereby making no distinction between  $T = 5/2$  and  $7/2$  states.

Zyskind *et al.* (1978) have published an excitation function for the 1529 and 2565 keV  $\gamma$  rays, in addition to a total  $(p, \gamma)$  cross section curve, over an energy range similar to that covered by the present experiment. A comparison of the respective yield curves shows excellent agreement in absolute magnitude and also in the correspondence between fine and gross structure.

### Statistical Model

The aim of the present study is to compare the predictions of Hauser-Feshbach statistical model calculations with experimental data for a reaction characterized by a large threshold effect. Full details of the calculations performed in the Melbourne laboratory with the computer code HAUSER\*4 have been given by Mann (1976), Christensen *et al.* (1977) and Switkowski *et al.* (1978*b*). The parameters which enter into such a calculation include optical potentials and level densities. As described by Switkowski *et al.* (1978*b*), only global parameter sets are used and no adjustments are performed in order to optimize fits. Such an approach is motivated by the realization that extensive statistical model calculations often need to be performed in stellar nucleosynthesis networks, where it is sensible to rely on only a single global set of parameters.

Inspection of the level scheme of Fig. 1 shows that the data available for discrete levels are sufficient for the calculated results to be insensitive to the details of the level density parameterization, which is invoked by the computer code once discrete level information is exhausted. All calculations include width fluctuation corrections (Tepel *et al.* 1974; Fowler 1978).

A distinctive feature of HAUSER\*4 is its ability to compute the cross sections for the production by the  $(p, \gamma)$  reaction of individual  $\gamma$  rays once branching ratio data are included (Mann 1976; Mann and Schenter 1977). The results of such statistical model calculations with global parameter sets are shown by the full curves in Fig. 3. The agreement between theory and experiment can be seen to be impressive, with the theory following the experimental data over the cross section range 2–300  $\mu\text{b}$  to within a factor of two. Similar correspondence for the total  $(p, \gamma)$  cross section has also been noted (Zyskind *et al.* 1978).

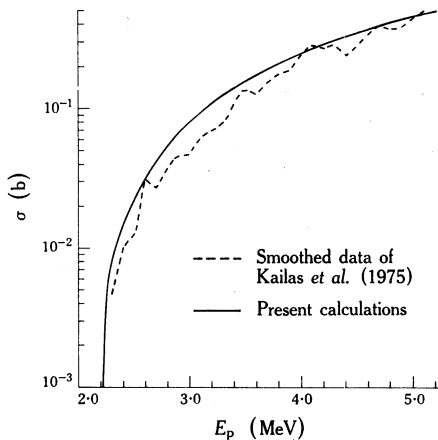


Fig. 4. Comparison between smoothed experimental data (dashed curve) and statistical model calculations (full curve) for the proton energy  $E_p$  dependence of the cross section  $\sigma$  for the  $^{54}\text{Cr}(p, n)^{54}\text{Mn}$  reaction.

In view of the success of the model in predicting the effects of neutron competition on the  $(p, \gamma)$  yield, it is interesting to compare the predicted  $(p, n)$  cross section with the results of experiment. A detailed  $(p, n)$  excitation function has been reported by Kailas *et al.* (1975) and their data, which have been smoothed for convenience of presentation, are represented by the dashed curve in Fig. 4. The statistical model predictions (shown by the full curve in Fig. 4) reproduce the data rather well.

In summary, the Hauser–Feshbach statistical model code HAUSER\*4, using global parameters, successfully describes both  $(p, \gamma)$  and  $(p, n)$  reactions for  $^{54}\text{Cr}$  at proton energies near the  $(p, n)$  threshold. There are now emerging systematics which attest to the accuracy of such model calculations for proton induced reactions on intermediate mass nuclei (Fowler 1978). Further experimental tests of the statistical model may now begin to address the hitherto neglected group of reactions including an  $\alpha$  particle in either the entrance or the exit channel.

#### Acknowledgments

We are grateful to Professor W. A. Fowler, Professor S. E. Woosley, Dr R. A. Spear and Dr J. L. Zyskind for informative discussions and correspondence throughout this program of work. We appreciated the assistance of B. Szymanski and P. Menon in the running of the Pelletron accelerator, and the helpful advice of members

of the Pelletron accelerator group. One of us (Z.E.S.) acknowledges receipt of a Queen Elizabeth II Fellowship. The work was supported by the Australian Research Grants Committee (Grant No. B77/15413).

### References

- Bock, R., Duhm, H. H., Martin, S., Rudel, R., and Stock, R. (1965). *Nucl. Phys. A* **72**, 273.
- Christensen, P. R., Switkowski, Z. E., and Dayras, R. A. (1977). *Nucl. Phys. A* **280**, 189.
- Fowler, W. A. (1976). Proc. 4th Conf. on Applications of Small Accelerators (Eds J. L. Duggan and I. L. Morgan), p. 11 (IEEE: New York).
- Fowler, W. A. (1978). Nuclear astrophysics. Caltech preprint No. OAP-526.
- Kailas, S., *et al.* (1975). *Phys. Rev.* **12**, 1789.
- Kennett, S. R., Switkowski, Z. E., Paine, B. M., and Sargood, D. G. (1979). *J. Phys. G* **5**, 399.
- Kuehn, P. R., O'Donnell, F. R., and Kobisk, E. H. (1972). *Nucl. Instrum. Meth.* **102**, 403.
- Mann, F. M. (1976). Hanford Engineering and Development Laboratory, Rep. No. HEDL-TME-7680.
- Mann, F. M., Dayras, R. A., and Switkowski, Z. E. (1975). *Phys. Lett. B* **58**, 420.
- Mann, F. M., and Schenter, R. E. (1977). *Nucl. Sci. Eng.* **63**, 242.
- Moses, J. D., Newson, H. W., Bilpuch, E. G., and Mitchell, G. E. (1971). *Nucl. Phys. A* **175**, 556.
- Solomon, S. B., and Sargood, D. G. (1978). *Nucl. Phys. A* **312**, 140.
- Switkowski, Z. E., Heggie, J. C., and Mann, F. M. (1978a). *Phys. Rev. C* **18**, 153.
- Switkowski, Z. E., Heggie, J. C., and Mann, F. M. (1978b). *Aust. J. Phys.* **31**, 253.
- Tepel, J. W., Hoffman, H. M., and Wiedenmüller, H. A. (1974). *Phys. Lett. B* **49**, 1.
- Wigner, E. P. (1948). *Phys. Rev.* **73**, 1002.
- Woosley, S. E., Fowler, W. A., Holmes, J. A., and Zimmerman, B. A. (1975). Tables of thermonuclear reaction rate data for intermediate mass nuclei. Caltech preprint No. OAP-422.
- Zyskind, J. L., *et al.* (1977). Proc. Int. Conf. on Nuclear Structure, Tokyo (Ed. T. Marumori), p. 846 (International Academic Printing: Tokyo).
- Zyskind, J. L., *et al.* (1979). *Nucl. Phys. A* **315**, 430.
- Zyskind, J. L., Davidson, J. M., Esat, M. T., Shapiro, M. H., and Spear, R. H. (1978). *Nucl. Phys. A* **301**, 179.

Manuscript received 15 January 1979